Modelling for semiconductor spintronics

S. Saikin, Y.V. Pershin and V. Privman

Abstract: The authors summarise semiclassical modelling methods, including drift-diffusion, kinetic transport equation and Monte Carlo simulation approaches, utilised in studies of spin dynamics and transport in semiconductor structures. As a review of the work by the authors' group, several examples of applications of these modelling techniques are presented.

1 Introduction

The idea to use the spin property of electrons in semiconductor electronic devices (semiconductor spintronics) is considered as one of the promising trends for future electronics [1, 2]. It is expected that utilisation of spin-related phenomena in information processing will extend the functionality of conventional devices and allow development of novel electronic devices based on new operating principles [3–9]. Recent interest has been motivated by successful examples of metallic spintronic devices, such as ferromagnetic metal-based reading heads for hard disc drives and magnetic random access memory. Possible applications of semiconductor spintronics include magnetic sensing and nonvolatile magnetic memory. In comparison with metal-based spintronics, reviewed e.g. in [10], utilisation of semiconductor structures promises more versatile design due to the ability to adjust potential variation and spin polarisation in the device channel by external voltages, device structure and doping profiles. Different types of devices [11–25] have been proposed recently. However, the actual advantages of most of these designs as compared to the conventional electronics devices have not been clearly established [26]. For example, the most promising proposal for an electronic analogue of an electro-optical modulator [13], that was later termed 'spin-field-effect transistor', has been criticised in [27]. To resolve this controversy a substantial basic research effort is required. Device design plays an important role in this problem [24, 25].

Recent experimental advances have allowed generation and control of nonequilibrium spin polarisation in semiconductor structures [4–9]. For example, it has been demonstrated that spin polarisation can be maintained [28] for up to several nanoseconds at room temperature and efficiently controlled by gate voltage [29] in GaAs (110) quantum wells. Coherent injection of polarised spins across material interfaces [30] and coherent transport of spin polarisation in homogeneous materials for a distance longer than 100 μm [31] have been reported. Some of the experiments go beyond the application of conventional electronic devices. It has been shown that spin-polarised current can reduce the threshold of a semiconductor laser up to 50% [32]. Information about electron spin polarisation can be transmitted to photon polarisation [19] and decoded by a detecting device [33]. More sophisticated experiments can control pure spin currents without charge currents in bulk semiconductors [34].

The goal of this paper is to review spin transport modelling approaches in the semiclassical, high-temperature regime of spatial transport, appropriate for operation of conventional devices of interest in electronics.

2 Spin dynamics of charge carriers

Spin, $\boldsymbol{s}$, is a quantum mechanical property, associated with intrinsic angular momentum vector of electrons, and many other elementary particles, as well as nuclei and atoms. An intrinsic magnetic moment is associated with spin, therefore spin is closely related to magnetic phenomena. However, the quantum mechanical nature of the spin makes it different from the classical angular momentum. The most important difference is that the spin is strongly quantised and can only take on discrete values. Its vector components do not commute with each other, therefore, electron spin requires, in most cases, a fully quantum-mechanical treatment. A natural constant which arises in the treatment of magnetic properties of electrons (spin 1/2 particles) is the Bohr magneton, $\mu_B = 9.274 \times 10^{-24}$ J/T.

In semiconductor spintronic structures, where spin is carried by electrons and/or holes, the spin dynamics is controlled by magnetic interactions. Some of these are surveyed in the following.

2.1 Interaction with an external magnetic field

An external magnetic field $\vec{B}$ exerts a torque on a magnetic dipole and the magnetic potential energy is given by Zeeman term

$$U = \frac{g^* \mu_B}{2} \vec{\sigma} \cdot \vec{B} \tag{1}$$

where g^* is the effective g-factor, and $\vec{\sigma}$ represents a vector of the Pauli spin matrices, used in the quantum-mechanical treatment of spin 1/2, see [35]. The interaction (1) leads to the spin precession around the external magnetic field. This interaction is important in all systems where a magnetic field is present. Moreover, fluctuations of $\vec{B}$ could lead to noise contributing to spin relaxation.

IEE Proceedings online no. 20045225

doi:10.1049/ip-cds:20045225

Paper first received 30th December 2004 and in revised form 31st March 2005

The authors are with the Center for Quantum Device Technology, Clarkson University, Potsdam, NY, 13699-5721, USA

S. Saikin is also with the Department of Theoretical Physics, Kazan State University, Kazan 420008, Russia

Y.V. Pershin is also with the Department of Physics and Astronomy, Michigan State University, East Lansing, Michigan 48824-2320, USA

E-mail: pershin@pa.msu.edu

2.2 Interaction with magnetic impurities, nuclei and other spin carriers

An electron located in a semiconductor experiences different kinds of spin-spin interactions including direct dipole-dipole interactions with nuclear spins and other (free and localised) electrons, and the exchange interaction. The latter, in fact, is the result of the electrostatic Coulomb interaction between electrons, which becomes spin-dependent because of the Pauli exclusion principle [35]. Usually, at room temperatures in sufficiently clean, low-doped nonmagnetic semiconductors these interactions are not very important.

2.3 Spin-orbit interaction

The spin-orbit (SO) interaction arises as a result of the magnetic moment of the spin coupling to its orbital degree of freedom. It is actually a relativistic effect, which was first found in the emission spectra of hydrogen. An electron moving in an electric field, experiences in its rest frame, an effective magnetic field. This field, which is dependent on the orbital motion of the electron, interacts with the electron's magnetic moment.

The Hamiltonian describing SO interaction, derived from the four-component Dirac equation [36], has the form:

$$H_{\mathrm{SO}} = \frac{\hbar^2}{4m^2c^2}\left(\vec{\nabla}V \times \vec{p}\right)\cdot\vec{\sigma} \tag{2}$$

where m is the free electron mass, $\vec{p}$ is the momentum operator, and $\vec{\nabla}V$ is the gradient of the potential energy, proportional to the electric field acting on the electron. When dealing with crystal structures, the spin-orbit interaction (2) accounts for symmetry properties of materials. Here, we emphasise two specific mechanisms that are considered to be important for spintronics applications. The Dresselhaus spin-orbit interaction [37] appears as a result of the asymmetry present in certain crystal lattices, e.g. the zinc blende structures. For a two-dimensional electron gas in semiconductor heterostructures with an appropriate growth geometry, the Dresselhaus SO interaction is of the form:

$$H_{\mathrm{D}} = \frac{\beta}{\hbar}(\sigma_x p_x - \sigma_y p_y) \tag{3}$$

Here, β is the coupling constant.

The Rashba spin-orbit interaction [38] arises due to the asymmetry associated with the confinement potential and is of interest because of the ability to electrically control the strength of this interaction. The latter is utilised, for instance, in the Datta-Das spin transistor [13]. The Hamiltonian for the Rashba interaction is written [38] as

$$H_{\mathrm{R}} = \frac{\alpha}{\hbar}\left(\sigma_x p_y - \sigma_y p_x\right) \tag{4}$$

where α is the coupling constant.

Other possible sources of spin-orbit interaction are nonmagnetic impurities, phonons [39], sample inhomogeneity, surfaces and interfaces. In some situations these could play a role in spin transport and spin relaxation dynamics.

In general, transport in semiconductor spintronic devices can be characterised by the creation of a nonequilibrium spin polarisation in the device (spin injection), measurement of the final spin state (spin detection), external control of the spin dynamics by the electric (gate modulation) or magnetic fields, and uncontrolled spin dynamics leading to loss of information in the device (spin relaxation or spin dissipation). Specifically, once injected into a semiconductor, electrons experience spin-dependent interactions with the environment, which cause spin relaxation. The spin polarisation in a typical semiconductor at room temperature is then lost over distances no larger than a fraction of 1 μm. This has been the main reason that the development of semiconductor spintronics is closely linked with the advent of nanotechnology, and spin-dependent phenomena in transport will play any role only when device components reach truly deep-sub-micron dimensions.

3 Drift-diffusion approach

The drift-diffusion approximation is the simplest approach to spin involving process modelling. Based on the well-known drift-diffusion model used to describe phenomena related only to the charge degree of freedom, drift diffusion models accounting for the spin degree of freedom can be subdivided into two classes: two-component drift-diffusion approximations and spin-polarisation-vector or density-matrix based models. Both approaches have been used successfully in practical modelling of spin-related phenomena in semiconductors [40–52]. General conditions for the applicability of these approximations are not different from the usual conditions of applicability of drift-diffusion approximations.

3.1 Two-component drift-diffusion model

The two-component drift-diffusion approach, originally devised for spin transport modelling in ferromagnetic metals, has been applied to spin-related problems in semiconductors [40–46, 52]. This model ignores the transverse spin coherence; spin relaxation processes are included phenomenologically. Generally, the electrons are considered to be of two types: having spin up or down. Drift-diffusion equations for each type of electron, including the relaxation terms, can be formulated as follows:

$$e\frac{\partial n_{\uparrow(\downarrow)}}{\partial t} = div\,\vec{j}_{\uparrow(\downarrow)} + \frac{e}{2\tau_{sf}}\left(n_{\downarrow(\uparrow)} - n_{\uparrow(\downarrow)}\right) + S_{\uparrow(\downarrow)}(\vec{r},t) \tag{5}$$

$$\vec{j}_{\uparrow(\downarrow)} = \sigma_{\uparrow(\downarrow)}\vec{E} + eD\nabla n_{\uparrow(\downarrow)} \tag{6}$$

and

$$\sigma_{\uparrow(\downarrow)} = en_{\uparrow(\downarrow)}\mu \tag{7}$$

where $-e$ is the electron charge, $n_{\uparrow(\downarrow)}$ is the density of the spin-up (spin-down) electrons, $\vec{j}_{\uparrow(\downarrow)}$ is their current density, τ_{sf} is the spin relaxation time, $S_{\uparrow(\downarrow)}(\vec{r},t)$ describes the source of the spin polarisation, $\sigma_{\uparrow(\downarrow)}$ is the conductivity and μ is the mobility, connected with the diffusion coefficient D via the Einstein relation $\mu = De/(k_BT)$, and defined via $\vec{v}_{drift} = \mu\vec{E}$.

Equation (5) is the usual continuity relation that takes into account spin relaxation and sources of the spin polarisation, (6) is the expression for the current which includes the drift and diffusive terms, and (7) is the expression for the conductivity. It is assumed that the diffusion coefficient D and the spin relaxation time τ_{sf} are equal for the spin-up and spin-down electrons. Equations (5)–(7) can be supplemented by the Poisson equation accounting for, for example, the effects of a non-homogeneous electric field,

$$div\,\vec{E} = \frac{e}{\varepsilon\,\varepsilon_0}(N - n) \tag{8}$$

Here, N is the positive background charge density and $n = n_\downarrow + n_\uparrow$ is the electron density. From (5)–(8), we obtain an equation for the spin polarisation density $P = n_\uparrow - n_\downarrow$,

$$\frac{\partial P}{\partial t} = D\Delta P + D\frac{e\vec{E}}{k_BT}\nabla P + D\frac{e\nabla\vec{E}}{k_BT}P - \frac{P}{\tau_{sf}} + F(\vec{r},t) \tag{9}$$

which can be supplemented by an equation for the electric field [43]. Here, $F(\vec{r},t) = \left[S_{\uparrow}(\vec{r},t) - S_{\downarrow}(\vec{r},t)\right]/e$ represents a spin polarisation density being created by the external source.

3.2 Accumulation of electron spin polarisation at semiconductor interfaces

Let us consider an example of using the two-component drift-diffusion model to describe propagation of electron spin polarisation through an interface separating two n-type semiconductor regions in an applied electric field [46]. We assume that an inhomogeneous spin polarisation is created locally by a continuous source and is driven through a boundary by an electric field, see Fig. 1*a*. Each semiconductor region is characterised by the following parameters: the diffusion coefficient D_i, doping level N_i and spin relaxation time τ_i. Neglecting the effect of charge redistribution at the interface (this effect was studied in [43]), the evolution of the electron spin polarisation is described in each semiconductor by (9). These equations were solved analytically with appropriate boundary conditions, representing flux conservation and continuity of spin polarisation density at the interface [46].

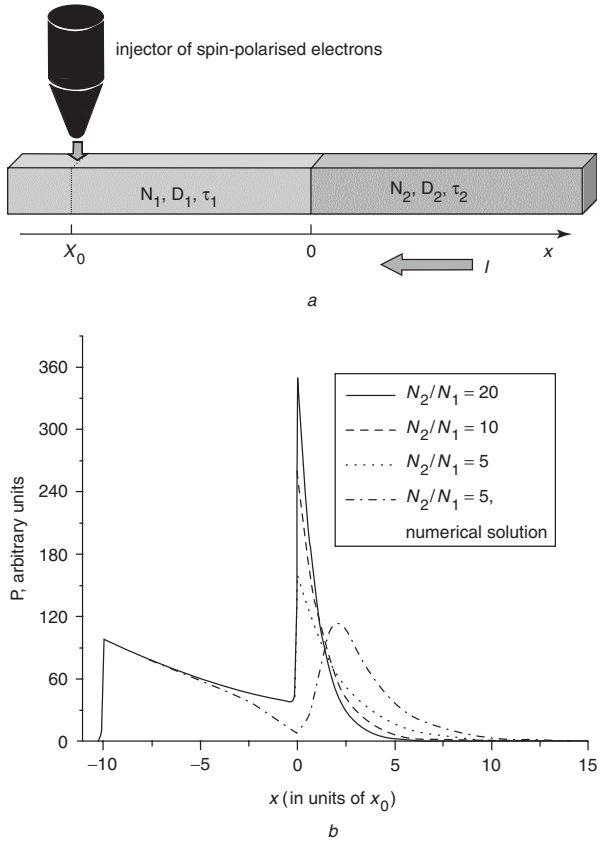

Fig. 1 *Propagation of spin-polarised electrons through a boundary between two n-type semiconductors*

a Schematic diagram of the system: spin-polarised electrons are injected at $x = x_0$ and move toward the interface located at $x = 0$, under the action of the electric field

b Spin polarisation density created by a point source at $x_0 = -10$, as a function of x for different doping densities N_2, with $\tau_1 = \tau_2$ and $D_1 = D_2$, showing the increase of the spin accumulation with higher N_2. The dash-dotted line represents the spin polarisation density obtained with taking into account additionally the redistribution of the electron density near the boundary, as detailed in [43]

It was found that, for certain values of parameters describing the system, the electron spin polarisation is accumulated near the interface. An example of such a situation is shown in Fig. 1*b*, where accumulation of the electron spin polarisation at the interface is more pronounced with increase of the doping density N_2. Qualitatively, this effect occurs because of the lower drift velocity in the higher doped region, resulting in deceleration of spin-polarised electrons after passing the interface and, correspondingly, in their accumulation. To avoid confusion, it should be emphasised that this method allows increasing the electron spin polarisation density $n_{\uparrow} - n_{\downarrow}$, but not the level of the electron spin polarisation, defined as $(n_{\uparrow} - n_{\downarrow})/(n_{\uparrow} + n_{\downarrow})$. Moreover, we wish to note here that the spin polarisation density is continuous at the interface; its sharp decrease in the left region near the interface is described by a fast decaying function [46]. It was shown in [46] that, to obtain a high level of the spin polarisation density at the interface, it is necessary that both semiconductors have long electron-spin relaxation times; the right semiconductor should have small electron diffusion coefficient and high doping level.

3.3 Gate control of spin polarisation drag in semiconductor heterostructures

We consider an example of modelling of a gate operation in a nonballistic spin FET [15]. The proposed device consists of a gated heterostructure with ferromagnetic source and drain contacts. The device utilises spin relaxation of conduction electrons in a semiconductor quantum well (QW) modulated by the gate voltage [15]. Spin-polarised electrons, injected from the source, propagate in the plane of the QW, formed in the heterostructure, and are filtered by the drain contact. The spin dynamics of the conduction electrons is controlled by the spin-orbit interaction. It was shown, theoretically, that, for some particular configurations, spin-polarised electrons can be transported without substantial loss of polarisation if the spin-orbit coupling coefficients α and β are nearly equal [15, 47, 53]. However, if the spin-orbit constants are made not equal, for example by applying an external electric field orthogonal to the QW plane, the spin dephasing mechanism [54] is efficient. As a result, a different spin polarisation of electrons in the device channel near the magnetic drain contact is produced. The magnetoresistance of the structure, and therefore the current through the device, is dependent on the value of this spin polarisation and its relative orientation with respect to the magnetization of the drain.

We can show that spin density along the channel for this example decays exponentially [47] as

$$P(x) = P(0)\mathrm{e}^{-x/L_s} \tag{10}$$

with the characteristic spin scattering length

$$L_s = \left(\frac{\mu E}{2D} + \sqrt{\left(\frac{\mu E}{2D}\right)^2 + \left(\frac{2m^*(\alpha(V_g) - \beta(V_g))}{\hbar^2}\right)^2} \right)^{-1} \tag{11}$$

where spin-orbit coefficients are functions of the gate voltage. These coefficients can be calculated based on the device material band structure [52]. For different values of the gate voltage, the spin density in the channel varies due to the change of the electron concentration and due to the modulation of the spin dephasing. To characterise the efficiency of the latter mechanism, spin polarisation should be used, normalised to the number of the electrons. Using realistic material parameters it is possible to establish that

the modulation of the spin polarisation in a submicrometre-sized AlGaAs/GaAs gated heterostructure at room temperature, within a reasonable range of the gate voltages, is of the order of 15–20% [52]. This effect can be observed experimentally. However, for a device application, further improvements of the structure design are desirable.

3.4 Spin polarisation vector approach

As an extension of the previously discussed model this approach accounts for the transverse spin dynamics [47–51]. This is important if time scales of processes studied are comparable with a characteristic decoherence/dephasing time for quantum-mechanical superposition of spin-up and spin-down states. For example, this transport regime can be exploited for spintronic devices operating with analogue logic [55]. The spin polarisation density, $\boldsymbol{P}$, in this case is a vector quantity. It corresponds to a single-particle spin density matrix as

$$\rho_\sigma = \frac{1}{2}\begin{pmatrix} 1+P_z & P_x - iP_y \\ P_x + iP_y & 1-P_z \end{pmatrix} \tag{12}$$

It should be noted that this representation (12) is still a single-electron description. For example, it cannot describe spin entanglement of two electrons. Under the assumption that the spin degree of freedom does not affect the spatial motion, it is possible to show that the dynamics of spin polarisation density are described by a vector drift-diffusion equation. For example, in the one-dimensional (1D) case it is [47, 49]

$$\frac{\partial \boldsymbol{P}}{\partial t} - \hat{\boldsymbol{D}}\frac{\partial^2 \boldsymbol{P}}{\partial x^2} - \hat{\boldsymbol{\mu}}\frac{\partial \boldsymbol{P}}{\partial x} + \hat{\boldsymbol{C}}\boldsymbol{P} = 0 \tag{13}$$

The coefficients $\hat{\boldsymbol{D}}$, $\hat{\boldsymbol{\mu}}$, $\hat{\boldsymbol{C}}$, in (13), are 3×3 matrixes in the spin space. The symmetry of these coefficients is defined by the properties of specific spin-dependent interactions. In general, all three matrix coefficients cannot be diagonalised simultaneously and equations for the components of the spin polarisation density vector cannot be decoupled.

3.5 Short-time approximation

In many applications, it is important to find the spatial distribution of the spin polarisation, $\boldsymbol{P}(\boldsymbol{r}, t)$, at an arbitrary moment of time t given the initial spin polarisation distribution $\boldsymbol{P}(\boldsymbol{r}, 0)$. Initial dynamics of the spin polarisation distribution can be found using the short-time approximation [50]. Within this approximation, $\boldsymbol{P}(\boldsymbol{r}, t)$ in the two-dimensional heterostructure geometry is given by

$$\boldsymbol{P}(x, y, t) = \iint G(x - x', y - y', t)\boldsymbol{P}'_{(x,y),(x',y')}dx'dy' \tag{14}$$

where $G(x - x', y - y', t)$ is the diffusion Green's function (solution of the diffusion equation with a point source), and $\boldsymbol{P}'_{(x,y),(x',y')}$ represents the contribution of the initial spin polarisation density at the point (x', y') to $\boldsymbol{P}(x, y, t)$. The structure of (14) can be easily understood. Electron spin polarisation density in a space volume with co-ordinates (x, y) at a selected moment of time t is given by a sum of the spin polarisation vectors of all the electrons located in this volume. The diffusion Green's function $G(x - x', y - y', t)$ gives the probability for the electrons to diffuse from the point (x', y') to (x, y), while $\boldsymbol{P}'_{(x,y),(x',y')}$ describes the spin polarisation of these electrons.

For the initial spin relaxation dynamics, the main approximations used to make (14) tractable are the assumptions that different spin rotations commute with each other and that the spin precession angle φ is proportional to the distance between (x', y') and (x, y). These assumptions are justified when the spin precession angle per mean free path is small and the time is short. Moreover, it is assumed that evolution of the electron spin degree of freedom is superimposed on the space motion of the charge carriers. In other words, the influence of the spin-orbit interaction on the spatial motion is neglected. If $\boldsymbol{a}$ is the unit vector along the precession axis, then [50]

$$\boldsymbol{P}'_{(x,y),(x',y')} = \boldsymbol{P} + \boldsymbol{P}_\perp(\cos\varphi - 1) + \boldsymbol{a} \times \boldsymbol{P}\sin\varphi \tag{15}$$

where $\boldsymbol{P}_\perp = \boldsymbol{P} - \boldsymbol{a}(\boldsymbol{aP})$ is the component of the spin polarisation perpendicular to the precession axis, $\varphi = \eta r$, while η is the spin precession angle per unit length, $\boldsymbol{r} = (x - x', y - y')$, and $r = |\boldsymbol{r}|$. Here $\boldsymbol{P} = \boldsymbol{P}(\boldsymbol{r}, t = 0)$. With only the Rashba spin-orbit interaction, $\boldsymbol{a} = \hat{z} \times \boldsymbol{r}/r$, and $\hat{z}$ is the unit vector in the z direction, perpendicular to QW. The definition of $\boldsymbol{a}$ in a more general case is given in [49]. It should be emphasised that the spin-orbit interaction is the origin of the spin polarisation rotations described by (15). The short-time approximation was used [50] in the investigation of the spin relaxation dynamics near the edge of two-dimensional electron gas (2DEG).

3.6 Anisotropy of spin transport in 2DEG

A specific form of the coefficients, $\hat{\boldsymbol{D}}$, $\hat{\boldsymbol{\mu}}$, $\hat{\boldsymbol{C}}$, in the drift-diffusion equation for the spin polarisation vector can be obtained by different methods [47, 49]. For example, to describe spin dynamics in 2DEG, controlled by the spin-orbit interaction, Equations (3)–(4), we can apply the moments expansion procedure to the Wigner function equation (see Section 4) [47]. In this case the coefficients, $\hat{\boldsymbol{D}}$, $\hat{\boldsymbol{\mu}}$, $\hat{\boldsymbol{C}}$, are as follows:

$$\hat{\boldsymbol{D}} = \begin{pmatrix} D & 0 & 0 \\ 0 & D & 0 \\ 0 & 0 & D \end{pmatrix},$$

$$\hat{\boldsymbol{\mu}} = \begin{pmatrix} \mu E & 2B_{xz}D & 0 \\ -2B_{xz}D & \mu E & 0 \\ 0 & 0 & \mu E \end{pmatrix},$$

$$\hat{\boldsymbol{C}} = \begin{pmatrix} D(B_{xz}^2 + B_{yz}^2) & -\mu E B_{xz} & -B_{yx}B_{yz}D \\ \mu E B_{xz} & D(B_{xz}^2 + B_{yx}^2 + B_{yz}^2) & 0 \\ -B_{yx}B_{yz}D & 0 & DB_{yx}^2 \end{pmatrix} \tag{16}$$

where D and μ are the diffusion coefficient and mobility of the carriers, E is the electric field in-plane of the QW, and B_{ij} describe the effects of the spin-orbit interactions. The latter parameters are functions of the spin-orbit coupling coefficients α and β, and the transport direction with respect to the crystallographic axes [47]. The evolution of the spin polarisation vector is characterised by the dissipation (loss of the spin polarisation) due to random spatial motion of carriers and superimposed coherent spin precession. The symmetry of the first mechanism is specified by the geometry of the structure, while the latter is determined by the directions of applied fields. The spin dynamics in such a system can be strongly anisotropic [15, 53, 56]. For example, for a QW grown in the (001) direction, if the spin-orbit coupling constants α and β are equal, the spin dissipation is suppressed for electrons propagating along the $(1\bar{1}\,0)$ direction. For an arbitrary orientation of the electron transport, and $\alpha = \beta$, the solution for the spin polarisation

density in an appropriately selected co-ordinate system can be represented as [47]

$$\begin{aligned} P_x(x) &= P_x(0)\mathrm{e}^{-\left(\frac{\mu E}{2D}+\sqrt{\left(\frac{\mu E}{2D}\right)^2+B_{yz}^2}\right)x}\cos(B_{xz}x), \\ P_y(x) &= P_y(0)\mathrm{e}^{-\left(\frac{\mu E}{2D}+\sqrt{\left(\frac{\mu E}{2D}\right)^2+B_{yz}^2}\right)x}\sin(B_{xz}x), \\ P_z(x) &= P_z(0)\mathrm{e}^{-\left(\frac{\mu E}{2D}+\left|\frac{\mu E}{2D}\right|\right)x} \end{aligned} \tag{17}$$

where the angular dependence is hidden in the coefficients B_{ij}. According to (17), for the z-component of the spin-polarisation density the spin relaxation is suppressed. The transverse component of the spin polarisation rotates about the effective magnetic field with the spin precession length, $L_\mathrm{p} = 2\pi/B_{xz}$, and decays with the spin dephasing length

$$L_\perp = \left(\frac{\mu E}{2D}+\sqrt{\left(\frac{\mu E}{2D}\right)^2+B_{yz}^2}\right)^{-1} \tag{18}$$

In Fig. 2, calculated angular dependencies of the spin precession and spin dephasing lengths are shown for a 10 nm AlGaAs/GaAs/AlGaAs QW. The in-plane electric field in this case affects the spin dephasing mechanism only. Within the utilised model, the spin dephasing is suppressed if the applied electric field is along the $(1\bar{1}0)$ direction. The frequency of the coherent spin precession is maximal in this case.

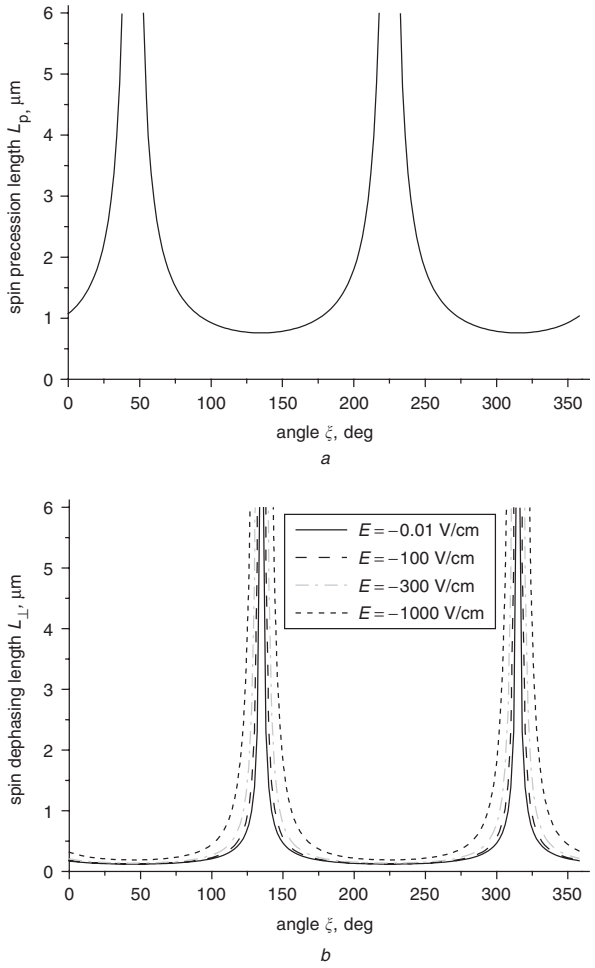

Fig. 2 *Spin precession length (a), and transverse spin dephasing length (b) for different transport orientations with respect to the (001) crystallographic direction at room temperature*

4 Kinetic transport equations

Similarly to charge transport, it is possible to describe transport of spin polarisation using Boltzmann-like kinetic equations. This can be done within the density matrix approach [57], or methods of nonequilibrium Green's functions [58, 59], or Wigner functions [60, 47], where spin property is accounted for starting from quantum mechanical equations. For example, spin-dependent interactions can be described using the method of invariants [61]. In this method, effects of nonequilibrium spin polarisation and/or external magnetic fields naturally appear in the effective mass Hamiltonian as corrections of the same order of magnitude as the effect of conduction band nonparabolicity. The transport equations accounting for spin polarisation can be represented as a set of equations for a spin distribution function (for spin 1/2, it is a set of three equations) plus equation for particle distribution function. The latter can be also represented by a set of equations if several types of carriers are utilised. In the general case, these equations are coupled.

In this Section, we consider a set of kinetic equations for transport of spin-polarised electrons in a semiconductor QW with spin dynamics controlled by the spin-orbit interaction, Equations (3)–(4). It can be derived based on the Wigner function approach [47, 60]. In the effective mass approximation, the single electron Hamiltonian is

$$H = \frac{\boldsymbol{p}^2}{2m^*} + V(\boldsymbol{r}) + H_\mathrm{SO},\ H_\mathrm{SO} = \boldsymbol{p}\cdot\bar{\boldsymbol{M}}\cdot\boldsymbol{\sigma}/\hbar \tag{19}$$

where $\boldsymbol{p}$ is the electron momentum, $V(\boldsymbol{r})$ corresponds to the interaction with an electric field oriented in the plane of the QW. The correction due to the spin-orbit interaction, H_SO, is written in a form, linear in electron momentum, where $\bar{\boldsymbol{M}}$ is a matrix (dyadic) of coupling coefficients [47]. Contribution to the Hamiltonian (19) due to interaction of the α-component of an electron momentum with β-component of its spin is proportional to the matrix element $M_{\alpha\beta}$. For simplicity, we consider transport of electrons in the one subband approximation with parabolic energy dispersion. The Wigner function for a single electron with spin is [60]

$$W_{s's}(\boldsymbol{R},\boldsymbol{k},t) = \int \psi^*(\boldsymbol{R}-\Delta\boldsymbol{r}/2,s')\psi(\boldsymbol{R}+\Delta\boldsymbol{r}/2,s)e^{-i\boldsymbol{k}\Delta\boldsymbol{r}}d^2\Delta r \tag{20}$$

where $\psi(r,s)$ is an electron wave function. In the spin space, the Wigner function (20) is a 2×2 matrix. It can be projected to the set of Pauli matrixes σ_α, and the unit matrix I, as [62]

$$W = \frac{1}{2}(W_n I + W_{\sigma_\alpha}\sigma_\alpha) \tag{21}$$

where W_n corresponds to the nonpolarised and W_{σ_α} corresponds to the α-component of the spin-polarised Wigner function. Following the standard procedure of transformation of the Schrödinger equation with the Hamiltonian (19) to the equation for the Wigner function [63], and assuming that the potential $V(\boldsymbol{r})$ varies slowly and smoothly with the position $\boldsymbol{r}$, we can obtain the transport equation for a single electron with spin

$$\frac{\partial W}{\partial t} + \frac{1}{2}\left\{v_j, \frac{\partial W}{\partial x_j}\right\} - \frac{1}{\hbar}\frac{\partial V}{\partial x_j}\frac{\partial W}{\partial k_j} + ik_j\left[v_j, W\right] = \mathrm{St}\,W \tag{22}$$

where $v_j = \partial H/\partial p_j$ is the velocity operator. At the right-hand side of (22), the phenomenological scattering term StW is included. The form of this term can be rather complicated and include transitions between different spin states [57, 59]. Operations [A,B] and {A,B} denote commutator and anticommutator, respectively.

Analytical solutions of a set of spin-polarised transport equations can be found for very simple cases only [60]. For quasi-equilibrium transport, approximate solutions can be obtained by an iteration procedure [57] or within a moment expansion scheme [47, 58]. If the transport regime is far from equilibrium or when electron-electron interactions have to be included, numerical solution schemes [59, 64] can be utilised.

5 Monte Carlo approach

The Monte Carlo simulation approach is one of most powerful methods to study characteristics of transport beyond quasi-equilibrium approximations, such as drift-diffusion or linear response approximations. This method has been widely used for modelling of charge carrier transport in semiconductor structures and modern devices [65–67]. Owing to its flexibility the approach can easily accommodate in different combinations details of scattering mechanisms, specific device design, material properties and boundary conditions in the simulation (for details see [67]). However, models designed for quantitative evaluations of transport parameters can be rather time consuming and require a lot of computational resources. Hence, in many applications where qualitative description of spin-dependent phenomena is required, simplified simulation schemes are useful.

The conventional ensemble Monte Carlo scheme utilised for electronic device design describes transport of classical 'representative' particles. Usually, each simulated particle represents a group of real electrons or holes with similar characteristics. In simulation, between scattering events, each particle propagates along a classical 'localised' trajectory and is affected by external fields. The electric interaction between charge carriers can be accounted for in the mean field approximation. In this case the electric field generated by the nonuniform charge distribution is recalculated every sampling time step using the Poisson equation. The simulation is carried out in a stepwise procedure that consists of 'free flight' of a particle in constant external fields, according to the classical equations of motion and instantaneous update of external fields at sampling events or update of the energy and momentum of a particle at scattering events. The scattering events are determined by defects, phonons, device geometry etc., with corresponding scattering rates given by the Fermi golden rule.

The spin property can be incorporated into this scheme easily as an additional parameter, spin polarisation vector [68] or spin density matrix [69] calculated for each particle. If spin-dependent interactions between the carriers (dipole-dipole interaction, exchange interaction) are small, then each spin can be considered separately driven by external fields or affected by spin-dependent scattering. Hence, spin dynamics of each particle can be simulated within the stepwise scheme described in the preceding paragraph. In the density matrix representation, during the free flight, the spin density matrix of the ith particle evolves coherently according to

$$\rho_i(t+\delta t) = e^{-\frac{iH_S\delta t}{\hbar}}\rho_i(t)\,e^{\frac{iH_S\delta t}{\hbar}} \tag{23}$$

where H_S is the (spin-dependent) Hamiltonian, assumed constant for short time steps, and it changes, instantaneously,

$$\rho_i(t) \rightarrow \rho_i'(t) \tag{24}$$

at spin scattering events.

As characteristic parameters, we can use the spin polarisation density,

$$P_\alpha = \sum_i Tr(\sigma_\alpha \rho_i) \tag{25}$$

and spin current densities [70]

$$J_\alpha^\beta = \sum_i v_\beta^i Tr(\sigma_\alpha \rho_i) \tag{26}$$

where v_β^i is the β velocity component of ith particle, and sums are taken over all particles located in the grid element of volume dV, at the position $\boldsymbol{r}$. These quantities, (25) and (26), can be also given in a normalised form [70] as

$$\begin{aligned} P_\alpha &= \sum_i Tr(\sigma_\alpha \rho_i) \Big/ \sum_i Tr(\rho_i), \\ X_\alpha^\beta &= \sum_i v_\beta^i Tr(\sigma_\alpha \rho_i) \Big/ \sum_i v_\beta^i Tr(\rho_i) \end{aligned} \tag{27}$$

With some variations, the described scheme has been successfully utilised to study different properties of spin transport in semiconductors during the past several years [68–83]. Most of the investigations were devoted to properties of electron spin-polarised transport in semiconductor heterostructures, where spin dynamics are driven by the spin-orbit interaction [68–77, 79, 81–83]. Among different aspects addressed in these studies were the effect of an electric gate on the coherent precession of spin polarisation in a semiconductor QW [68] and influence of device geometry (effects of width [71, 72], length [69], nano-patterns [73], crystallographic symmetry [53], contact/device interface [70, 82]) on spin evolution. Investigation of spin transport properties in semiconductor nanowires has been carried out in [74–76], where the authors studied spin dephasing [74, 75] and spin noise [76] in a high field transport regime using a multiple-subband model. Details of the precessional spin dephasing were investigated in [50, 77, 78, 83]. An approach to suppressing the effect of spin dephasing was proposed in [79], where it was shown that the electron spin relaxation time depends on the initial spin polarisation profile and a specific structure, a 'spin-coherence standing wave', has a several times longer spin relaxation time than the homogeneous electron spin polarisation.

In the referenced works, the spin dynamics were described by coherent evolution of spin during free flight of carriers according to (23), while scattering events were assumed spin independent. An example of Monte Carlo simulation of spin-polarised transport, where spin dynamics are controlled by spin scattering events can be found in [80]. In all the discussed studies, the back reaction of the spin motion on the particle spatial motion was neglected.

5.1 Relaxation of electron spin polarisation near the edge of 2DEG

According to the preceding discussion, spin transport modelling can be, generally, separated into two parts: simulation of electron spatial motion (usually, neglecting the spin degree of freedom) and calculation of the corresponding spin dynamics. The electron space motion can be considered at different levels of complexity. Clearly, the most detailed approach gives the most exact predictions and precise results. However, in most applications high precision is not as important as the speed of the calculations. In this Subsection we consider an example based on a simplified consideration of the electron spatial motion and density-matrix approach to the spin. This

method was originally proposed in [72]. It was subsequently used for studies of spin relaxation in 2DEG with an antidot lattice [73], dynamics of spin relaxation near the edge of the 2DEG [50], control of spin polarisation by pulsed magnetic fields [83], and investigation of long-lived spin coherence states [79].

Within the Monte Carlo simulation algorithm, the space motion of the 2DEG electrons is considered to be along classical (linear) trajectories interrupted by the bulk scattering events. The modelling involves spin-independent bulk scattering processes, which could be caused, for example, by phonon scatterings or impurities. For the sake of simplicity, the scattering due to such events is assumed to be elastic and isotropic, i.e. the magnitude of the electron velocity is conserved in the scattering events, while the final direction of the velocity vector is randomly selected. The time scale of the bulk scattering events can then be fully characterised by a single rate parameter, the momentum relaxation time τ_p. It is connected to the mean free path by $L_p = v\tau_p$. Here, v is the mean electron velocity. The dynamics of the spin degree of freedom, described by the polarisation vector $\boldsymbol{P}$, in the presence of spin-orbit interactions, reduces to precessions about an effective momentum-dependent magnetic field.

At the initial moment of time, the electron co-ordinates and direction of velocity are randomly generated, while the spin direction is selected according to initial conditions. The main loop of the Monte Carlo simulation algorithm involves the following steps: generation of a time interval between two consecutive scattering events, calculation of the spin dynamics (using the spin polarisation vector equation of motion), and random generation of a new direction of the electron velocity after scattering.

The D'yakonov-Perel' (DP) spin relaxation mechanism [84] is the leading spin relaxation mechanism in many important experimental situations. In the framework of the DP theory, the initial electron spin polarisation relaxes with time. The DP theory was formulated for the bulk of a sample. Considering electron spin relaxation near the edge of 2DEG, we would expect a similar relaxation scenario. This expectation, however, is not correct. Recent studies [50] have demonstrated that the spin relaxation dynamics near the edge is rather unusual and cannot be described by a simple exponential law, as follows from the DP theory. The described Monte Carlo simulation algorithm was used complementary to analytical investigation of short-time spin-relaxation dynamics [50]. Figure 3 shows the electron spin polarisation at different moments of time. Whereas the electron spin polarisation exponentially decreases in the bulk region, its behaviour near the edge is rather unusual. Longer spin relaxation time near the edge, spin polarisation oscillations and spin polarisation transfer from the perpendicular to in-plane component were observed.

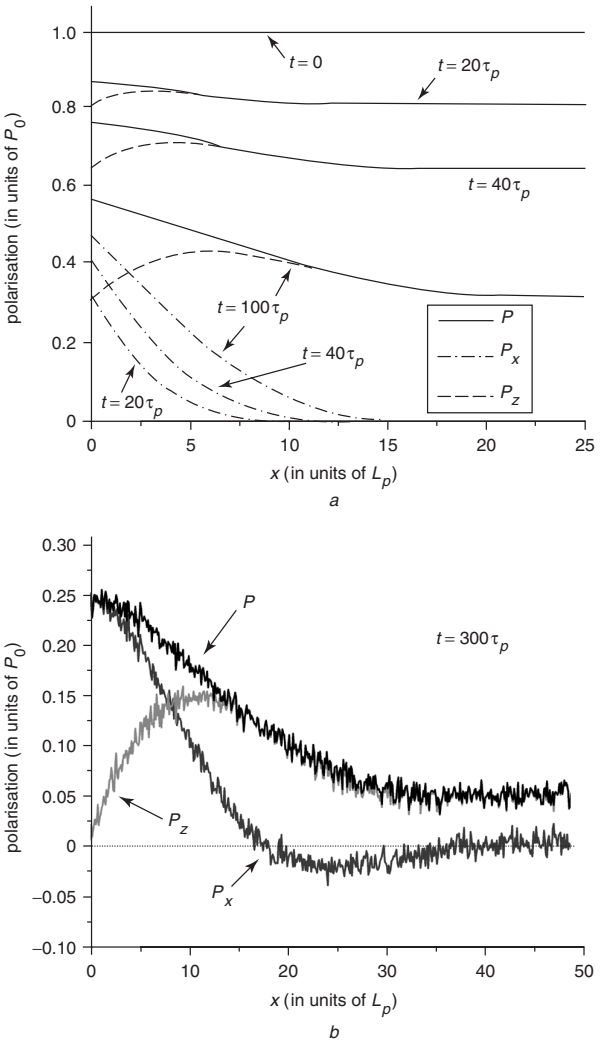

Fig. 3 *Short-time (a) and long-time (b) evolution of electron spin polarisation near the edge of 2DEG*
Suppression of spin relaxation near the edge, as well as spin oscillations in time and space were found

5.2 Spin-polarised transport in a finite length device structure

The size of modern semiconductor devices is submicron [1]. In such structures the average electric field can easily reach several kV/cm, and transport of charge carriers is characterised by nonequilibrium charge distribution, potential profile, electron energy etc. To study spin dynamics in such a regime, transport of spin-polarised electrons in an asymmetric quantum well formed in a $In_{0.52}Al_{0.48}As/In_{0.53}Ga_{0.47}As/In_{0.52}Al_{0.48}As$ semiconductor heterostructure, Fig. 4, has been simulated using an ensemble Monte Carlo scheme [81].

The length of the device was taken as $l = 0.55\,\mu m$. For study of spin transport, the width was assumed infinite,

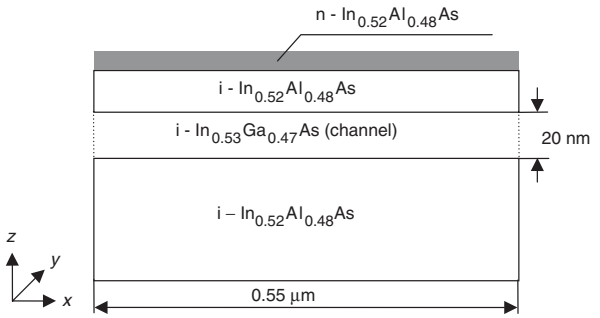

Fig. 4 *Schematic diagram of the device simulated*

neglecting effects of a finite device width studied in [71, 72]. The boundary conditions were specified by the following rules. Thermalised electrons were generated at the left (source) boundary. The charge neutrality of the whole device was conserved during the simulation. Once an electron left the device, a new particle was introduced at the source boundary. Initially, injected particles were assumed 100% spin-polarised in a specific direction of polarisation. The spin polarisation of a single electron was defined by the

single electron spin density matrix (12). The particle transport was simulated consistently by using the Poisson equation to update the charge distribution along the device channel. The spin dynamics were evaluated for each single particle using (23), where the spin-dependent Hamiltonian H_S was represented by two spin-orbit terms (3) and (4). In this case, (23) involves

$$e^{-iH_S\delta t/\hbar} = \begin{pmatrix} \cos(|\gamma|\delta t) & i\,\dfrac{\gamma}{|\gamma|}\sin(|\gamma|\delta t) \\ i\,\dfrac{\gamma^*}{|\gamma|}\sin(|\gamma|\delta t) & \cos(|\gamma|\delta t) \end{pmatrix} \qquad (28)$$

and its Hermitian conjugate. The parameter γ is determined by spin-orbit coupling constants and an electron momentum as

$$\gamma = \hbar^{-1}\left[\left(\alpha k_y + \beta k_x\right) + i\left(\alpha k_x + \beta k_y\right)\right] \qquad (29)$$

In the simulation, the total number of representative particles was $N = 55000$, and the sampling time step was $\Delta t_{samp} = 1$ fs. The program was run for 20000 time steps to achieve the steady-state transport regime, and then data were collected during the last 2000 time steps.

As shown in Fig. 5, the electrons injected with the average thermal energy 26 meV are rapidly heated up if the voltage $V_{DS} = 0.1$–0.25 V is applied along the device channel. The electron concentration is nearly constant in the channel, except for a small accumulation region (~ 0.01 μm) that is defined by the boundary conditions. Figure 6 illustrates that the spin dephasing in the structure is somewhat dependent on the applied voltage and temperature. Similar features have been emphasised in [74] where spin transport in GaAs nanowires was studied.

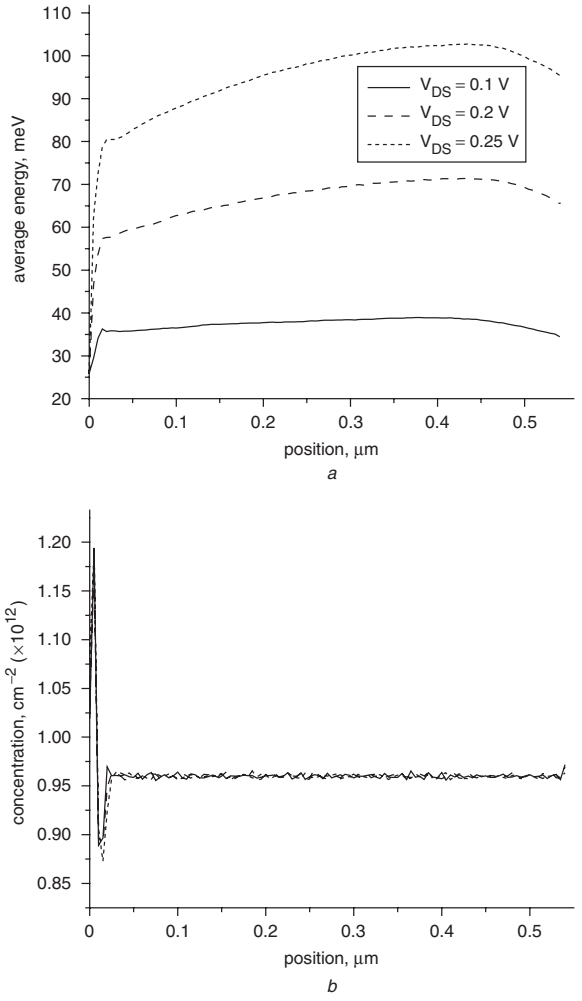

Fig. 5 *Energy profile (a) and electron concentration (b) along the device channel for different values of drain/source voltage for $T = 300$ K*

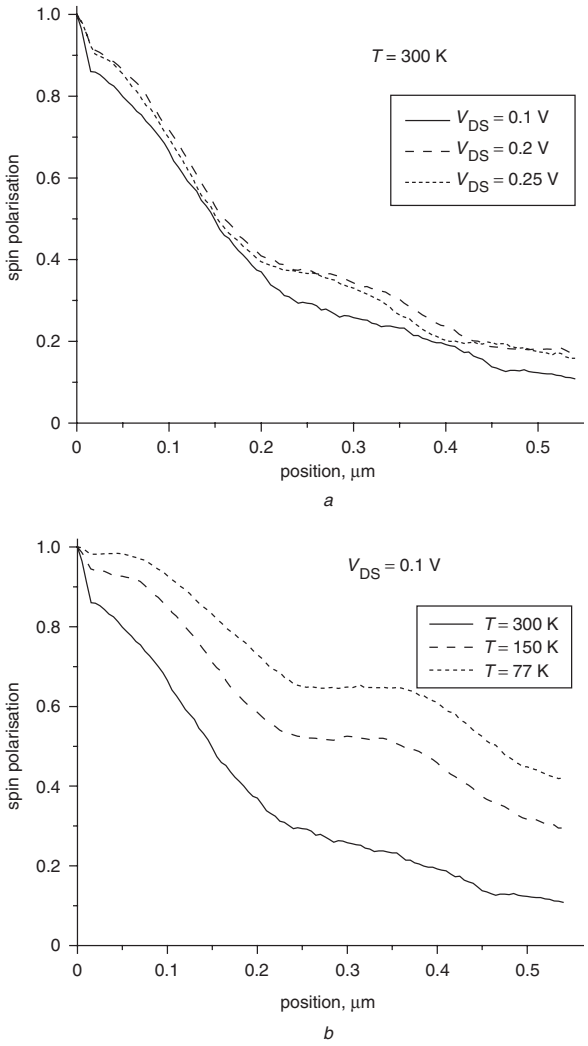

Fig. 6 *Distribution of spin polarisation*
a For different values of drain/source voltage, at $T = 300$ K
b For different temperatures for $V_{DS} = 0.1$ V

5.3 Spin injection through a Schottky barrier

The problem of spin injection into a nonmagnetic semiconductor is one of the important issues of semiconductor spintronics. Design of most of the proposed spintronic devices [13, 15–17, 19] requires an efficient source of spin-polarised carriers. Recently, it has been proven theoretically [85–87] and demonstrated experimentally [88–90] that spin-polarised electrons can be injected into a semiconductor from a metal ferromagnetic contact through a Schottky barrier. The Monte Carlo approach has been utilised to investigate spin dynamics in a device that consists of a ferromagnetic metal contact connected to a semiconductor heterostructure similar to that shown in Fig. 4 [70, 82]. In the metal part, the electrons are assumed to be spin-polarised with some distribution of polarisation as a function of the electron energy, while in the semiconductor

part of the device spin dynamics are controlled by the spin-orbit interaction. The conduction band profile of the considered device, calculated based on the electron concentration in a semiconductor with boundary conditions specified by the applied voltage is shown in Fig. 7. Owing to the potential barrier at the metal/semiconductor interface, the boundary conditions, corresponding to this design, are appreciably different from those utilised in the previous example. Details of the model can be found in [70].

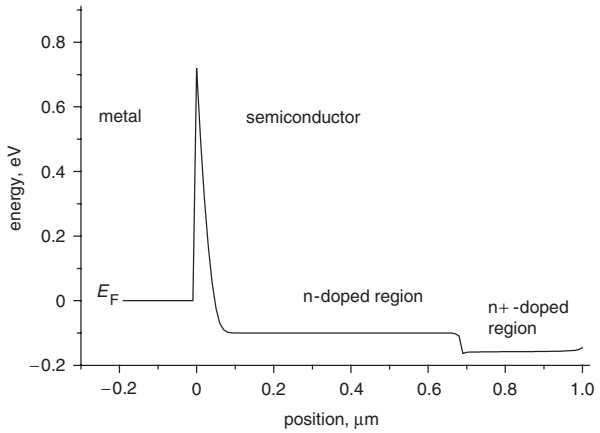

Fig. 7 *Simulated conduction band profile, $V_{DS} = 0.1$ V*

In the simulation, spin-polarised electrons are transported into the semiconductor by two different mechanisms, thermionic emission and tunnelling. Injected electrons represent only a small fraction of electrons in the semiconductor part. Hence, two types of representative particles, injected and persistently existing in the device channel, have been used in the model. In Fig. 8 the energy distribution of the injected electrons at bias voltage $V_{DS} = 0.1$ V at room temperature is shown. Owing to the high kinetic energy of electrons injected [70], the spin-orbit interaction was accounted for beyond the linear approximations, (3) and (4).

The particles persistently existing in the semiconductor part do not affect charge and spin current densities. However, they produce a nonpolarised background that suppresses the spin polarisation density, see (25), in the

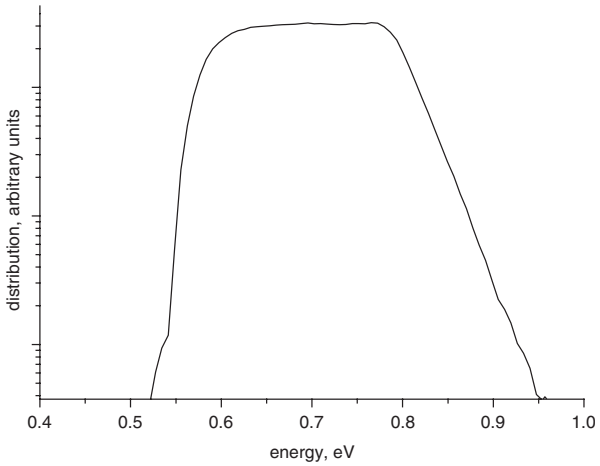

Fig. 8 *Energy distribution of electrons injected through the Schottky barrier, $V_{DS} = 0.1$ V, $T = 300$ K*

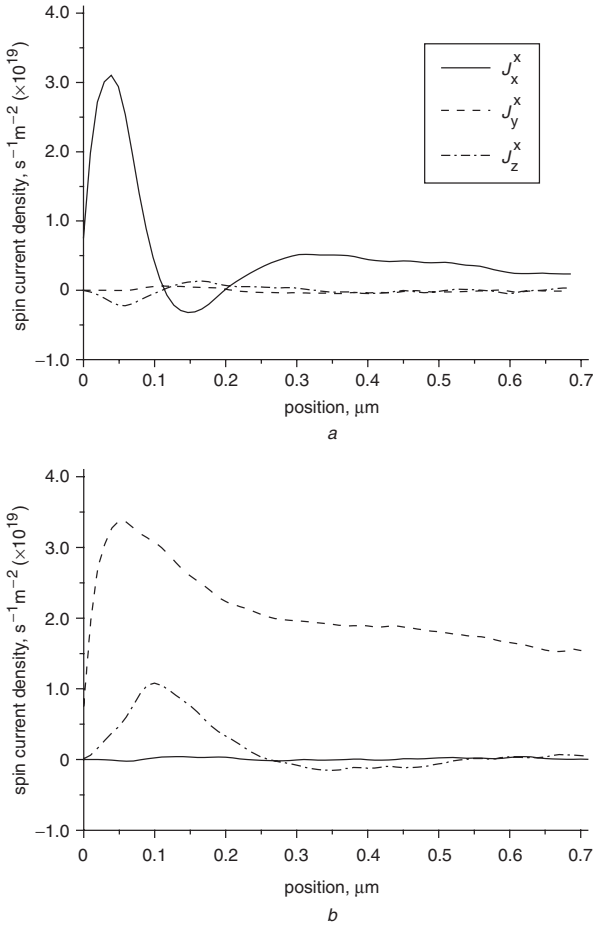

Fig. 9 *Spin current density for two orientations of spin injection*
a Injected polarisation is along the channel
b Injected polarisation is in the plane of the QW orthogonal to the channel

channel. Hence, the spin current density, see (26), was considered as a more useful characteristic of the spin dynamics in the structure. In Fig. 9, the spin current density is shown for two different orientations of the injected polarisation. Owing to spin dephasing, spin current is not conserved along the channel. The spin dynamics are strongly anisotropic with respect to the injected polarisation. It has been found that spin current polarised in the plane of the QW, orthogonal to the transport direction, is conserved for a longer distance [70]. It has also been shown that by n^+ doping of the Schottky barrier region spin current can be controlled over several orders of magnitude [82].

6 Acknowledgments

The authors gratefully acknowledge helpful discussions and collaboration with M.-C. Cheng, J.A. Nesteroff, E. Shafir, M. Shen and I.D. Vagner. This research was supported by the National Security Agency and Advanced Research and Development Activity under US Army Research Office contract DAAD-19-02-1-0035, and by the National Science Foundation, grant DMR-0121146.

7 References

1 International Technology Roadmap for Semiconductors (Ed. 2003), website http://public.itrs.net/Files/2003ITRS/Home2003.htm
2 'Research needs for novel devices' (SRC Edition, May 2003)

3 Prinz, G.: 'Spin-polarised transport', *Phys. Today*, 1995, **48**, (4), pp. 58–63
4 Wolf, S.A., Awschalom, D.D., Buhrman, R.A., Daughton, J.M., von Molnar, S., Roukes, M.L., Chtchelkanova, A.Y., and Treger, D.M.: 'Spintronics: a spin-based electronics. Vision for the future', *Science*, 2001, **294**, pp. 1488–1495
5 Das Sarma, S.: 'Spintronics', *Am. Sci.*, 2001, **89**, pp. 516–523
6 Awschalom, D.D., Flatte, M.E., and Samarth, N.: 'Spintronics', *Sci. Am.*, 2002, **286**, pp. 66–73
7 Akinaga, H., and Ohno, H.: 'Semiconductor spintronics', *IEEE Trans. Nanotechnol.*, 2002, **1**, pp. 19–31
8 Jonker, B.T.: 'Progress toward electrical injection of spin-polarised electrons into semiconductors', *Proc. IEEE*, 2003, **91**, pp. 727–740
9 Zutic, I., Fabian, J., and Das Sarma, S.: 'Spintronics: fundamentals and applications', *Rev. Mod. Phys.*, 2004, **76**, pp. 323–410
10 Parkin, S., Jiang, X., Kaiser, C., Panchula, A., Roche, K., and Samant, M.: 'Magnetically engineered spintronic sensors and memory', *Proc. IEEE*, 2003, **91**, pp. 661–680
11 Fabian, J., Zutic, I., and Das Sarma, S.: 'Magnetic bipolar transistor', *Appl. Phys. Lett.*, 2004, **84**, pp. 85–87
12 Flatte, M.E., Yu, Z.G., Johnson-Halperin, E., and Awschalom, D.D.: 'Theory of semiconductor magnetic bipolar transistors', *Appl. Phys. Lett.*, 2003, **82**, pp. 4740–4742
13 Datta, S., and Das, B.: 'Electronic analog of the electro-optic modulator', *Appl. Phys. Lett.*, 1990, **56**, pp. 665–667
14 Wang, B., Wang, J., and Guo, H.: 'Quantum spin field effect transistor', *Phys. Rev. B, Condens. Matter Mater. Phys.*, 2003, **67**, pp. 092408/1–4
15 Schliemann, J., Egues, J.C., and Loss, D.: 'Nonballistic spin-field-effect transistor', *Phys. Rev. Lett.*, 2003, **90**, pp. 146801/1–4
16 Egues, J.C., Burkard, G., and Loss, D.: 'Datta-Das transistor with enhanced spin control', *Appl. Phys. Lett.*, 2003, **82**, pp. 2658–2660
17 Wang, X.F., and Vasilopoulos, P.: 'Influence of subband mixing due to spin-orbit interaction on the transmission through periodically modulated waveguides', *Phys. Rev. B, Condens. Matter Mater. Phys.*, 2003, **68**, pp. 035305/1–8
18 Hall, K.C., Lau, W.H., Gundogdu, K., Flatte, M.E., and Boggess, T.F.: 'Non-magnetic semiconductor spin transistor', *Appl. Phys. Lett.*, 2003, **83**, pp. 2937–2939
19 Jonker, B.T.: 'Polarised optical emission due to decay or recombination of spin-polarised injected carriers'. 23 February 1999, US patent 5874749
20 Mani, R.G., Johnson, W.B., Narayanamurti, V., Privman, V., and Zhang, Y.-H.: 'Nuclear spin based memory and logic in quantum Hall semiconductor nanostructures for quantum computing applications', *Physica E*, 2002, **12**, pp. 152–156
21 Vrijen, R., Yablonovitch, E., Wang, K., Jiang, H.W., Balandin, A., Roychowdhury, V., Mor, T., and DiVincenzo, D.: 'Electron-spin-resonance transistors for quantum computing in silicon-germanium heterostructures', *Phys. Rev. A*, 2000, **62**, pp. 012306/1–10
22 Bandyopadhyay, S., and Cahay, M.: 'Proposal for a spintronic femto-Tesla magnetic field sensor', *Physica E*, 2005, **27**, pp. 98–103
23 Ciuti, C., McGuire, J.P., and Sham, L.J.: 'Spin-dependent properties of a two-dimensional electron gas with ferromagnetic gates', *Appl. Phys. Lett.*, 2002, **81**, pp. 4781–4783
24 Osipov, V.V., and Bratkovsky, A.M.: 'A class of spin injection-precession ultrafast nanodevices', *Appl. Phys. Lett.*, 2004, **84**, pp. 2118–2120
25 Bratkovsky, A.M., and Osipov, V.V.: 'High-frequency spin-valve effect in a ferromagnet-semiconductor-ferromagnet structure based on precession of the injected spins', *Phys. Rev. Lett.*, 2004, **92**, pp. 098302/1–4
26 D'yakonov, M.: 'Spintronics?', in Luryi, S., Xu, J. and Zaslavsky, A. (Eds.): 'Future trends in microelectronics: the nano, the giga and the ultra' (Wiley-IEEE Press, 2004)
27 Bandyopadhyay, S., and Cahay, M.: 'Reexamination of some spintronic field-effect device concepts', *Appl. Phys. Lett.*, 2004, **85**, pp. 1433–1435
28 Ohno, Y., Terauchi, R., Adachi, T., Matsukura, F., and Ohno, H.: 'Spin relaxation in GaAs (110) quantum wells', *Phys. Rev. Lett.*, 1999, **83**, pp. 4196–4199
29 Karimov, O.Z., John, G.H., Harley, R.T., Lau, W.H., Flatté, M.E., Henini, M., and Airey, R.: 'High temperature gate control of quantum well spin memory', *Phys. Rev. Lett.*, 2003, **91**, pp. 246601/1–4
30 Malajovich, I., Berry, J.J., Samarth, N., and Awschalom, D.D.: 'Persistent sourcing of coherent spins for multifunctional semiconductor spintronics', *Nature*, 2001, **411**, pp. 770–772
31 Kikkawa, J.M., and Awschalom, D.D.: 'Lateral drag of spin coherence in gallium arsenide', *Nature*, 1999, **397**, pp. 139–141
32 Rudolph, J., Hägele, D., Gibbs, H.M., Khitrova, G., and Oestreich, M.: 'Laser threshold reduction in a spintronic device', *Appl. Phys. Lett.*, 2003, **82**, pp. 4516–4518
33 Lannon, J.M., Dausch, D.E., and Temple, D.: 'High sensitivity polarized-light discriminator device', 24 April 2003, US patent application
34 Stevens, M.J., Smirl, A.L., Bhat, R.D.R., Najmaie, A., Sipe, J.E., and van Driel, H.M.: 'Quantum interference control of ballistic pure spin currents in semiconductors', *Phys. Rev. Lett.*, 2003, **90**, pp. 136603/1–4
35 Landau, L.D., and Lifshitz, E.M.: 'Quantum mechanics' (Butterworth-Heinemann, Oxford, 1997)
36 Condon, E.U., and Shortley, G.H.: 'The theory of atomic spectra' (Cambridge University Press, Cambridge, 1953)
37 Dresselhaus, G.: 'Spin-orbit coupling effects in zinc blende structures', *Phys. Rev.*, 1955, **100**, pp. 580–586
38 Bychkov, Yu., and Rashba, E.I.: 'Oscillatory effects and the magnetic susceptibility of carriers in inversion layers', *J. Phys. C*, 1984, **17**, pp. 6039–6045
39 Gantmakher, V.F., and Levinson, Y.B.: 'Carrier scattering in metals and semiconductors', in Agranovich, V.M. and Maradudin, A.A. (Eds.): 'Modern problems in condensed matter science' (North-Holland, New York, , 1987), Vol. 17
40 Yu, Z.G., and Flatté, M.E.: 'Spin diffusion and injection in semiconductor structures: Electric field effects', *Phys. Rev. B, Condens. Matter Mater. Phys.*, 2002, **66**, pp. 235302/1–14
41 Yu, Z.G., and Flatté, M.E.: 'Electric-field dependent spin diffusion and spin injection into semiconductors', *Phys. Rev. B, Condens. Matter Mater. Phys.*, 2002, **66**, pp. 201202/1–4
42 Žutič, I., Fabian, J., and Das Sarma, S.: 'Spin-polarised transport in inhomogeneous magnetic semiconductors: theory of magnetic/nonmagnetic *p-n* junctions', *Phys. Rev. Lett.*, 2002, **88**, pp. 066603/1–4
43 Pershin, Y.V., and Privman, V.: 'Focusing of spin polarisation in semiconductors by inhomogeneous doping', *Phys. Rev. Lett.*, 2003, **90**, pp. 256602/1–4
44 Pershin, Y.V., and Privman, V.: 'Propagation of spin-polarised electrons through interfaces separating differently doped semiconductor regions'. Proc. Conf. IEEE-NANO 2003 (IEEE Press, Monterey, CA, 2003), pp. 168–170
45 Martin, I.: 'Spin-drift transport and its applications', *Phys. Rev. B, Condens. Matter Mater. Phys.*, 2003, **67**, pp. 014421/1–5
46 Pershin, Y.V.: 'Accumulation of electron spin polarisation at semiconductor interfaces', *Phys. Rev. B, Condens. Matter Mater. Phys.*, 2003, **68**, pp. 233309/1–4
47 Saikin, S.: 'Drift-diffusion model for spin-polarised transport in a non-degenerate 2DEG controlled by a spin-orbit interaction', *J. Phys. Condens. Matter*, 2004, **16**, pp. 5071–5081
48 Culcer, D., Sinova, J., Sinitsyn, N.A., Jungwirth, T., MacDonald, A.H., and Niu, Q.: 'Semiclassical spin transport in spin-orbit-coupled bands', *Phys. Rev. Lett.*, 2004, **93**, pp. 046602/1–4
49 Pershin, Y.V.: 'Drift–diffusion approach to spin-polarised transport', *Physica E*, 2004, **23**, pp. 226–231
50 Pershin, Y.V.: 'Dynamics of spin relaxation near the edge of two-dimensional electron gas', *Physica E*, 2005, **27**, pp. 77–81
51 Burkov, A.A., Nunez, A.S., and MacDonald, A.H.: 'Theory of spin-charge-coupled transport in a two-dimensional electron gas with Rashba spin-orbit interactions', *Phys. Rev. B, Condens. Matter Mater. Phys.*, 2004, **70**, pp. 155308/1–8
52 Shafir, E., Shen, M., and Saikin, S.: 'Modulation of spin dynamics in a channel of a nonballistic spin-field effect transistor', *Phys. Rev. B, Condens. Matter Mater. Phys.*, 2004, **70**, pp. 241302(R)/1–4
53 Saikin, S., Shen, M., and Cheng, M.-C.: "Study of spin-polarised transport properties for spin-FET design optimization', *IEEE Trans. Nanotechnol.*, 2004, **3**, pp. 173–179
54 Dyakonov, M.I., and Kachorovskii, V.Y.: 'Spin relaxation of two-dimensional electrons in noncentrosymmertic semiconductors', *Sov. Phys. Semicond.*, 1986, **20**, pp. 110–112
55 Bauer, G.E.W., Tserkovnyak, Y., Huertas-Hernando, D., and Brataas, A.: 'From digital to analogue magnetoelectronics: theory of transport in non-collinear magnetic nanostructures' in 'Advances in Solid State Physics' (Springer-Verlag, Berlin, 2003), Vol. 43
56 Averkiev, N.S., and Golub, L.E.: 'Giant spin relaxation anisotropy in zinc-blende heterostructures', *Phys. Rev. B, Condens. Matter Mater. Phys.*, 1999, **60**, pp. 15582–15584
57 Ivchenko, E.L., Lyanda-Geller, Y.B., and Pikus, G.E.: 'Current of thermalized spin-oriented photocarriers', *Sov. Phys.-JETP*, 1990, **71**, pp. 550–557
58 Takahashi, Y., Shizume, K., and Masuhara, N.: 'Spin diffusion in a two-dimensional electron gas', *Phys. Rev. B, Condens. Matter Mater. Phys.*, 1999, **60**, pp. 4856–4865
59 Weng, M.Q., and Wu, M.W.: 'Kinetic theory of spin transport in *n*-type semiconductor quantum wells', *J. Appl. Phys.*, 2003, **93**, pp. 410–420
60 Mishchenko, E.G., and Halperin, B.I.: 'Transport equations for a two-dimensional electron gas with spin-orbit interaction', *Phys. Rev. B, Condens. Matter Mater. Phys.*, 2003, **68**, pp. 045317/1–6
61 Bir, G.L., and Pikus, G.E.: 'Symmetry and strain-induced effects in semiconductor' (Keter Publishing House Jerusalem Ltd., 1974)
62 Carruthers, P., and Zachariasen, F.: 'Quantum collision theory with phase-space distributions', *Rev. Mod. Phys.*, 1983, **55**, pp. 245–285
63 Wigner, E.: 'On the quantum correction for thermodynamic equilibrium', *Phys. Rev.*, 1932, **40**, pp. 749–759
64 Weng, M.Q., Wu, M.W., and Jiang, L.: 'Hot-electron effect in spin dephasing in n-type GaAs quantum wells', *Phys. Rev. B, Condens. Matter Mater. Phys.*, 2004, **69**, pp. 245320/1–9
65 Hess, K.: 'Monte carlo device simulation: full band and beyond' (Kluwer Academic Publishers, Boston, 1991)
66 Tomizawa, K.: 'Numerical simulation of submicron semiconductor devices' (Artech House, London, Boston, 1993)
67 Fischetti, M.V., and Laux, S.E.: 'DAMOCLES theoretical manual' (IBM, Yorktown Heights, 1995)
68 Bournel, A., Dollfus, P., Bruno, P., and Hesto, P.: 'Gate-induced spin precession in an $In_{0.53}Ga_{0.47}As$ two dimensional electron gas', *Eur. Phys. J. Appl Phys.*, 1998, **4**, pp. 1–4

69 Saikin, S., Shen, M., Cheng, M.-C., and Privman, V.: 'Semiclassical Monte Carlo model for in-plane transport of spin-polarised electrons in III–V heterostructures', *J. Appl. Phys.*, 2003, **94**, pp. 1769–1775
70 Shen, M., Saikin, S., and Cheng, M.-C.: 'Monte Carlo modelling of spin injection through a Schottky barrier and spin transport in a semiconductor quantum well', *J. Appl. Phys.*, 2004, **96**, pp. 4319–4325
71 Bournel, A., Dollfus, P., Bruno, P., and Hesto, P.: 'Spin-dependent transport phenomena in a HEMT', *Physica B*, 1999, **272**, pp. 331–334
72 Kiselev, A.A., and Kim, K.W.: 'Progressive suppression of spin relaxation in two-dimensional channels of finite width', *Phys. Rev. B, Condens. Matter Mater. Phys.*, 2000, **61**, pp. 13115–13120
73 Pershin, Y.V., and Privman, V.: 'Slow spin relaxation in two-dimensional electron systems with antidots', *Phys. Rev. B, Condens. Matter Mater. Phys.*, 2004, **69**, pp. 073310/1–4
74 Pramanik, S., Bandyopadhyay, S., and Cahay, M.: 'Spin dephasing in quantum wires', *Phys. Rev. B, Condens. Matter Mater. Phys.*, 2003, **68**, pp. 075313/1–10
75 Pramanik, S., Bandyopadhyay, S., and Cahay, M.: 'Decay of spin-polarised hot carrier current in a quasi-one-dimensional spin-valve structure', *Appl. Phys. Lett.*, 2004, **84**, pp. 266–268
76 Pramanik, S., and Bandyopadhyay, S.: 'Spin fluctuations and "spin noise" '. Proc. Int. Symp. on Clusters and Nano-Assemblies, Richmond, VA, USA, Nov. 2003
77 Bournel, A., Dollfus, P., Cassan, E., and Hesto, P.: 'Monte Carlo study of spin relaxation in AlGaAs/GaAs quantum wells', *Appl. Phys. Lett.*, 2000, **77**, pp. 2346–2348
78 Barry, E.A., Kiselev, A.A., and Kim, K.W.: 'Electron spin relaxation under drift in GaAs', *Appl. Phys. Lett.*, 2003, **82**, pp. 3686–3688
79 Pershin, Y.V.: 'Long-lived spin coherence states in semiconductor heterostructures', *Phys. Rev. B, Condens. Matter Mater. Phys.*, 2005, **71**, pp. 155317/1–5
80 Pershin, Y.V., and Privman, V.: 'Spin relaxation of conduction electrons in semiconductors due to interaction with nuclear spins', *Nano Lett.*, 2003, **3**, pp. 695–700
81 Shen, M., Saikin, S., Cheng, M.-C., and Privman, V.: 'Monte Carlo modelling of spin FETs controlled by spin-orbit interaction', *Math. Comput. Simul.*, 2004, **65**, pp. 351–363
82 Shen, M., Saikin, S., and Cheng, M.-C.: 'Spin injection in spin FETs using a step-doping profile', *IEEE Trans. Nanotechnol.*, 2005, **4**, pp. 40–44
83 Pershin, Y.V.: 'Spin coherence control by pulsed magnetic fields', e-print cond-mat/0310225
84 D'yakonov, M.I., and Perel, V.I.: 'Spin orientation of electronics associated with the interband absorption of light in semiconductors,', *Sov. Phys.-JETP*, 1971, **33**, pp. 1053–1059
85 Rashba, E.I.: 'Theory of electrical spin injection: Tunnel contacts as a solution of the conductivity mismatch problem', *Phys. Rev. B, Condens. Matter Mater. Phys.*, 2000, **62**, pp. R16267–R16270
86 Albrecht, J.D., and Smith, D.L.: 'Spin-polarised electron transport at ferromagnet/semiconductor Schottky contacts', *Phys. Rev. B, Condens. Matter Mater. Phys.*, 2003, **68**, pp. 035340/1–14
87 Osipov, V.V., and Bratkovsky, A.M.: 'Efficient nonlinear room-temperature spin injection from ferromagnets into semiconductors through a modified Schottky barrier', *Phys. Rev. B, Condens. Matter Mater. Phys.*, 2004, **70**, pp. 205312/1–6
88 Ploog, K.H.: 'Spin injection in ferromagnet-semiconductor heterostructures at room temperature', *J. Appl. Phys.*, 2002, **91**, pp. 7256–7260
89 Hanbicki, A.T., van't Erve, O.M.J., Magno, R., Kioseoglou, G., Li, C.H., Jonker, B.T., Itskos, G., Mallory, R., Yasar, M., and Petrou, A.: 'Analysis of the transport process providing spin injection through an Fe/AlGaAs Schottky barrier', *App. Phys. Lett.*, 2003, **82**, pp. 4092–4094
90 Adelmann, C., Lou, X., Strand, J., Palmstrøm, C.J., and Crowell, P.A.: 'Spin injection and relaxation in ferromagnet-semiconductor heterostructures', *Phys. Rev. B, Condens. Matter Mater. Phys.*, 2005, **71**, pp. 121301R/1–4